# Seismic Drift Demand and Capacity of Non-seismically Designed Concrete Buildings in Hong Kong

R.K.L. Su
*Department of Civil Engineering, Email*: klsu@hkucc.hku.hk
*The University of Hong Kong, Hong Kong, China*
N.T.K. Lam
*Department of Civil and Environmental Engineering*
*The University of Melbourne, Australia*
H.H. Tsang
*Department of Civil Engineering*
*The University of Hong Kong, Hong Kong, China*

ABSTRACT: This paper reviews the seismic engineering research conducted in Hong Kong with special emphasis on the prediction of the seismic drift demand and capacity of existing buildings which have not been designed and detailed to address potential seismic hazards. The paper begins with a comprehensive summary of the local construction and detailing practice of concrete structures, followed by a summary of the drift ratio capacity, ductility capacity, stiffness variation and non-linear damping properties of the non-seismically designed reinforced concrete components. Seismic design response spectra for rock sites developed from Chinese Code GB50011-2001 are compared with the uniform hazard response spectra developed at the University of Hong Kong. The over-conservatism of the Chinese Code particularly in the long period range (T > 2 sec) is highlighted. A direct displacement based method used for the prediction of the maximum drift demands of existing buildings in Hong Kong is also introduced. Phenomena such as stiffness degradation, period shifting, non-linear damping and higher mode effects have been incorporated into the modelling. Lastly, the predicted maximum inter-storey drift demand of 0.3% is compared with the minimum ultimate drift capacity of approximately 1.5%. The capacity predictions were based on results from experimental cyclic load testings of concrete sub-assemblages undertaken in Hong Kong in recent times. The potential risk of damage in Hong Kong buildings under seismic attacks is discussed.

KEYWORDS: Seismic drift demand, seismic drift capacity, inter-storey drift, existing buildings

## 1 INTRODUCTION

In the past, buildings in Hong Kong were designed in accordance with the British Standards. Only cyclonic wind loading as opposed to earthquake loading was taken into account in the design of the building despite that the region has been classified as "low-to-moderate seismicity". Thus, the potential structural performance of the non-seismically designed buildings in the projected earthquake scenarios for Hong Kong is a cause for concern. This prompted numerous investigations in recent years into the seismic drift capacity and the potential demand on existing buildings. Buildings subject to seismic actions would experience reversed cyclic swaying. Earthquake-induced deformations may be quantified by the roof displacement $\Delta_{roof}$ as well as the inter-storey displacement $\Delta_i$ as shown in Figure 1.

Inter-storey drift ratio at the $i^{th}$ floor can be defined as

$$\theta_i = \frac{\Delta_i}{h_i} \quad (1)$$

where $h_i$ is the storey height.

Past earthquake events demonstrated that the extent of damage to buildings is closely related to the inter-storey drift demand. Excessive inter-storey drift could cause damage to both the structural and non-structural components. Collapse of buildings is often resulted from the local concentration of deformation at a particular "weak storey". Both the inter-storey drift demand and the drift capacity of the lateral resisting elements in the building have been estimated, in accordance with results obtained from numerical simulations and experimental studies. The design response spectra associated with the projected critical

earthquake scenarios for the Hong Kong region were used for calculating the maximum inter-storey drift demands. Meanwhile, the seismic drift capacities of the key structural components, including columns and walls, were estimated from experimental data. The potential risk of drift induced damage in buildings when subject to earthquake induced ground shaking was then assessed.

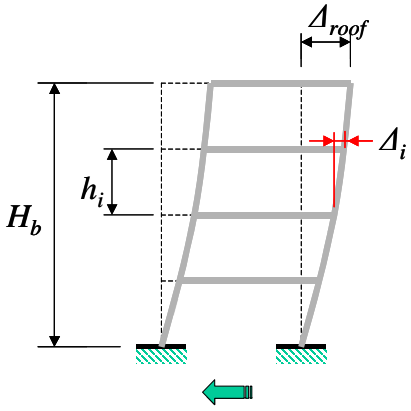


Figure 1. Roof displacement and inter-storey displacement.

## 2 DRIFT CAPACITY OF REINFORCED CONCRETE WALLS AND COLUMNS

Hong Kong is located in a region of low-to-moderate seismicity. Traditionally, the structural design of reinforced concrete (RC) buildings in Hong Kong had to follow certain British Standards, namely, BS8110 (BSI 1985), CP110 (BSI 1972) and CP114 (BSI 1969). Earthquake actions were not considered in the design based on these standards, and there were no explicit provisions for ensuring adequate ductility in the structure. The new concrete design code (BD 2004) which stipulates ductile RC detailing as a statutory requirement has only been implemented in 2004. Thus, the main bulk of the current building stock in Hong Kong was constructed without seismic resistant provisions. Addressing this, extensive experimental studies were conducted across different institutions in Hong Kong to investigate the seismic response behaviour of typical non-seismically designed RC structural components. In this section, the experimental work of Xiong (2001), Lam *et al.* (2003), Huang (2003), Li (2003), Ho (2003), Kuang and Wong (2005), Wong (2005), and Kuang and Ho (2005) on the non-seismically detailed structural members are reviewed. The variations of the drift ratio capacity, stiffness degradation and damping ratio together with the displacement ductility factor have been determined. These are the essential ingredients for the accurate predictions of the inelastic seismic response behaviour of buildings when subject to earthquake ground shaking.

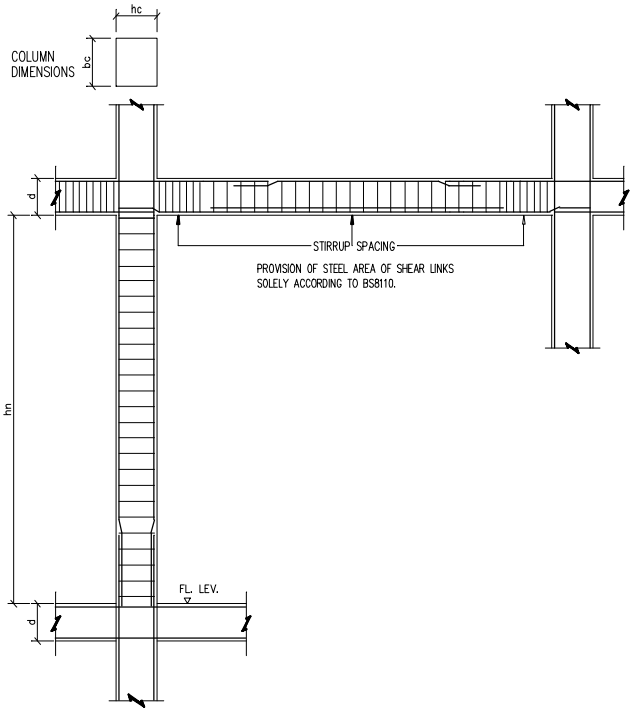


Figure 2. Typical non-seismic RC details of beam and column.

### 2.1 *Non-seismic R C details*

As British Standards do not limit the axial load ratio of vertical structural components, longitudinal steel ratios of columns (and walls) in Hong Kong buildings can go up to 6% (and 4%). Lappings of the longitudinal reinforcement are often located near the base of the columns and in the potential plastic hinge region (see Figure 2). In order to simplify the steel fabrication process and to reduce bar congestion, all the links (transverse reinforcement) are bent with 90° hooks. These links are not normally provided at the beam-column joints. British Standards BS8110 (1985) stipulates that the spacing of links in a column to be equal to or less than 300 mm, 12 times the bar diameter, or 0.75 times the depth of the section, whichever has the least dimension. Transverse ties in columns are therefore equally distributed with spacings of around 300 mm over the entire length of the column and closer link arrangements are not provided at the potential plastic hinge regions (near the beam-column joints). Thus the conditions of confinement in the concrete, the shear strength of the beam-column joints, and the ductility of the structure in a typical Hong Kong building are much inferior to that of a seismically designed building. A comparison of the seismically and non-seismically designed RC beam-column details adopted in the local construction industry in terms of their construction cost and time can be found in Su *et al.* (2001).

### 2.2 *Axial load ratio and steel ratios*

Axial load ratio and steel ratios are the main parameters affecting the ductility and drift ratio capacity of

structural members. The axial load ratio in a RC section is defined by equation (2).

$$n = \frac{P}{f_c' A_g} \tag{2}$$

Where $P$ is the axial load in the component concerned $f_c'$ is the concrete cylinder strength and $A_g$ is the gross sectional area of the concrete section.

The longitudinal reinforcement ratio refers to the amount of main reinforcement in a RC section, represented as a percentage of the gross sectional area ($A_g$). Since members such as walls and columns are always taking substantial amount of axial loads, this study does not distinguish "tension-taking" reinforcements from "compression-taking" reinforcements. Instead, the amount of reinforcement is represented by a single ratio as calculated by equation (3).

$$\rho_s = \frac{A_s}{A_g} = \frac{\sum A_{s,i}}{A_g} = \frac{\sum [(\pi \cdot d_{s,i}^2)/4]}{A_g} \tag{3}$$

where $d_s$ is the bar diameter, $A_s$ is the sectional area of longitudinal reinforcement.

The amount of transverse reinforcement in RC member may be quantified by the volumetric transverse reinforcement ratio, $\rho_{sh}'$ (Paulay and Priestley 1992), as defined by equation (4).

$$\rho_{sh}' = \frac{V_s}{A_c \cdot s} = \frac{\sum V_{s,i}}{A_c \cdot s} = \frac{\sum [(\pi \cdot d_{s,i}^2) \cdot l_{s,i}/4]}{A_c \cdot s} \tag{4}$$

where $s$ is the pitch of transverse reinforcement, $l_s$ is the length of the reinforcement, $A_c$ is the sectional area of the concrete core and $V_s$ is the volume of shear reinforcement.

Alternatively, the amount of transverse reinforcement in a RC member may be quantified by the transverse reinforcement ratio $\rho_{sh}$ (Lam *et al*. 2003) using equation (5).

$$\rho_{sh} = \frac{A_{sh}}{sh_c} \tag{5}$$

where $A_{sh}$ are the total area of transverse reinforcement perpendicular to the direction of the lateral load and $h_c$ is the depth of the member core (in the direction of the lateral load) measured centre-to-centre of the transverse reinforcement.

The transverse and longitudinal reinforcement can provide confinement to concrete. The effectiveness of the confinement can be quantified by the confinement effectiveness factor according to Sheikh and Uzumeri (1982) which is expressed as,

$$\alpha = \left(1 - \frac{s_t}{2b_c}\right)\left(1 - \frac{s_t}{2h_c}\right)\left(1 - \frac{\sum b_i^2}{6b_c h_c}\right) \tag{6}$$

where $b_c$ is the width of the member core measured centre-to-centre of the transverse reinforcement, and $b_i$ is the distance of successive longitudinal bars laterally restrained at stirrup corners by 135 degree hooks.

Su and Wong (2007) conducted a survey study in Hong Kong for 17 existing buildings. The range of axial load ratios in the core walls, shear walls and columns are listed in Table 1. It can be seen that the average axial load ratios at service load conditions are around 0.20 for walls and 0.36 for columns. At ultimate conditions, the axial load ratios for walls and columns can be increased to 0.50 and 0.87 respectively, Wong (2005) also determined the typical longitudinal and volumetric transverse reinforcement ratios in the wall and column members at their base level. Table 2 shows the percentages of longitudinal steel used in columns and shear walls. The rather high average value of 3.0% in columns and 1.89% in walls are noted. In comparison, the average volumetric transverse reinforcement ratio is only 0.35% in shear walls. In summary, concrete columns and walls in a typical Hong Kong building features high axial load ratio, high longitudinal steel ratio but a rather low volumetric transverse steel ratios. All these features point to a potentially non-ductile performance of the structure in extreme conditions.

Table 1. Axial load ratios at service load condition of members at the base level of the buildings.

| Structural members | Axial load ratio | | |
|---|---|---|---|
| | Minimum | Average | Maximum |
| Core Walls | 0.079 | 0.172 | 0.278 |
| Shear Walls | 0.116 | 0.198 | 0.327 |
| Columns | 0.205 | 0.363 | 0.572 |

Table 2. Longitudinal and transverse reinforcement ratios of members at the base level of the buildings.

| Structural members | Steel ratio (%) | |
|---|---|---|
| | Average | Range |
| Longitudinal reinforcement ratio | | |
| Core Walls | 2.06 | 0.37-3.75 |
| Shear Walls | 1.89 | 0.38-5.61 |
| Columns | 3.00 | 0.50-6.00 |
| Volumetric transverse reinforcement ratio | | |
| Core Walls | 0.31 | 0.17-0.46 |
| Shear Walls | 0.35 | 0.15-0.52 |

### 2.3 *Previous tests on non-seismic details*

Experimental testing of half-scale non-seismically designed RC columns and walls under various combinations of axial loads and longitudinal reinforcement ratios have been conducted in Hong Kong. Table 3 presents the geometric, loading and material parameters of the specimens. In this table, $f_{cu}$, $f_y$ and $f_{yh}$ denotes, respectively, the concrete cube strength, the yield stress of the longitudinal and transverse re-

inforcements in the specimens. Concrete grades ($f_{cu}$) ranging from 34-109 MPa and high tensile reinforcement was employed for fabricating the specimens. The shear span-to-depth ratios ranged from 1.0 to 5.1 and the breath-to-depth ratios ranged from 0.02 to 1. The axial load ratios of 0.1-0.44 for walls and 0-0.53 for columns were consistent with local construction practices. The longitudinal steel ratios ($\rho_s$) of 0.9-6.1% in the column specimens were also in good agreement with the observations (of 0.5-6%) from the previous survey. However, the longitudinal reinforcement ratios in the wall specimens were only in the narrow range of 0.92-2%. There has been a lack of test data for walls with low shear span-to-depth ratio ($m$) and high axial load ratio ($n$). Due to the space limitations of the paper, details of the experimental set-up and instrumentations are not presented herein.

Reversed cyclic loadings were applied to all of the listed specimens. The load-rotation curves were recorded in each case. Under high axial load ratios, failure of columns (Units BS-60-06-61S and BS-60-06-61C) was mainly due to the crushing of the concrete and the buckling of the longitudinal reinforcement. For shear walls under high axial load ratios, out-of-plane sliding failure was observed (with Unit W2).

Table 3. Geometric, loading and material parameters of the specimens (continued).

| Reference | Unit | *m* | *b/d* | *N* |
|---|---|---|---|---|
| Walls | | | | |
| Wong 2005 | W1 | 4.0 | 0.02 | 0.25 |
| | W2 | 4.0 | 0.02 | 0.44 |
| Kuang and Ho 2007 | UD-1.0 | 1.0 | 0.08 | 0.11 |
| | UD-1.5 | 1.5 | 0.08 | 0.10 |
| | CD-1.0 | 1.0 | 0.08 | 0.11 |
| | CD-1.5 | 1.5 | 0.08 | 0.10 |
| Columns | | | | |
| Xiong 2001 | X1 | 4.4 | 1.0 | 0.35 |
| | X2 | 4.4 | 1.0 | 0.17 |
| | X7 | 4.4 | 1.0 | 0.18 |
| Huang 2003 | E-0.0 | 3.4 | 1.0 | 0.00 |
| | E-0.3 | 3.4 | 1.0 | 0.30 |
| Lam et al. 2003 | X-7 | 3.0 | 1.0 | 0.45 |
| | X-9 | 1.5 | 1.0 | 0.40 |
| Li 2003 | E-C80-B80-0 | 3.4 | 1.0 | 0.00 |
| | E-C80-B40-0.2 | 3.4 | 1.0 | 0.20 |
| Ho 2003 | BS-60-06-61S | 5.1 | 1.0 | 0.53 |
| | BS-60-06-61C | 5.1 | 1.0 | 0.53 |
| | BS-100-03-24S | 5.1 | 1.0 | 0.28 |
| | BS-100-03-24C | 5.1 | 1.0 | 0.31 |
| | BS-80-01-09S(1) | 5.1 | 1.0 | 0.11 |
| | BS-80-01-09S(2) | 5.1 | 1.0 | 0.11 |
| | BS-80-01-09S(3)S | 5.1 | 1.0 | 0.11 |
| Kuang and Wong 2005 | NSD-200 | 4.5 | 1.0 | 0.20 |

## 2.4 *Yield drift ratio, ultimate drift ratio and ductility ratio*

There exists more than one definitions of yield displacement within the research community. The yield displacement may be determined in accordance with the equal energy area method (Lam *et al*. 2003), the "first yield" displacement of the reinforcement (Priestley 2000), the "first yield" displacement of the concrete (Li 2003), or a hypothetical yield point of an equivalent linearly elastic-perfectly plastic system (Kuang and Ho 2005, Ho 2003, Wong 2005).

The hypothetical yield point criterion has been used in this study to define the yield drift ratios for the specimens attributed to the simplicity of the approach. As illustrated in Figure 3, the yield displacement $\Delta_y$ is defined as the displacement of a hypothetical yield point of an equivalent linearly elastic-perfectly plastic system whose initial elastic stiffness and yield strength are respectively set equal to the secant stiffness at $0.75F_u$ and $F_u$. The yield displacement so evaluated is given by equation (7).

$$\Delta_y = \Delta'_y / 0.75 \tag{7}$$

where $\Delta'_y$ is the displacement at $0.75F_u$. The displacement ductility factor $\mu$ is defined by equation (8).

$$\mu = \Delta / \Delta_y \tag{8}$$

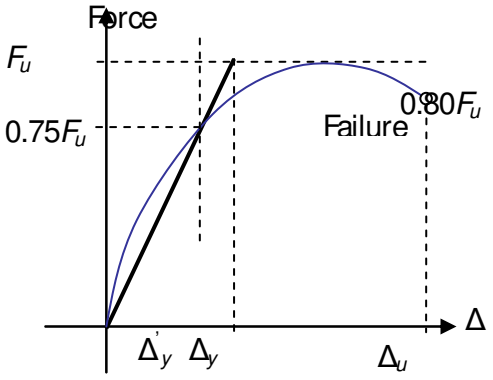


Figure 3. Definitions of yield and ultimate displacements.

The ultimate displacement $\Delta_u$ is the displacement at which the resisting force has dropped to 0.80 of the peak load-carrying capacity in the post-peak branch. Experimental results are presented in terms of the yield drift ratio $\theta_y$ and the ultimate drift ratio $\theta_u$ which is defined by equations (9) and (10) respectively.

Table 3. Geometric, loading and material parameters of the specimens.

| Reference | Unit | ρs (%) | ρ'sh (%) | ρsh (%) | α |
|---|---|---|---|---|---|
| Walls | | | | | |
| Wong 2005 | W1 | 2.00 | 0.54 | 0.28 | 0.19 |
| | W2 | 2.00 | 0.82 | 0.28 | 0.19 |
| Kuang and Ho 2007 | UD-1.0 | 0.92 | 1.81 | 0.92 | 0.29 |
| | UD-1.5 | 0.92 | 1.81 | 0.92 | 0.29 |
| | CD-1.0 | 0.92 | 1.88 | 0.92 | 0.29 |
| | CD-1.5 | 0.92 | 1.88 | 0.92 | 0.29 |
| Columns | | | | | |
| Xiong 2001 | X1 | 2.00 | 1.02 | 0.53 | 0.32 |
| | X2 | 2.00 | 0.58 | 0.30 | 0.32 |
| | X7 | 2.00 | 1.02 | 0.53 | 0.32 |
| Huang 2003 | E-0.0 | 3.60 | 0.38 | 0.16 | 0.36 |
| | E-0.3 | 3.60 | 0.38 | 0.16 | 0.36 |
| Lam et al. 2003 | X-7 | 3.53 | 0.67 | 0.29 | 0.36 |
| | X-9 | 3.03 | 0.32 | 0.14 | 0.36 |
| Li 2003 | E-C80-B80-0 | 3.60 | 0.38 | 0.16 | 0.35 |
| | E-C80-B40-0.2 | 3.60 | 0.38 | 0.16 | 0.31 |
| Ho 2003 | BS-60-06-61S | 6.10 | 0.38 | 0.19 | 0.34 |
| | BS-60-06-61C | 6.10 | 0.47 | 0.20 | 0.41 |
| | BS-100-03-24S | 2.40 | 0.66 | 0.34 | 0.30 |
| | BS-100-03-24C | 2.40 | 0.66 | 0.28 | 0.22 |
| | BS-80-01-09S(1) | 0.90 | 0.38 | 0.19 | 0.18 |
| | BS-80-01-09S(2) | 0.90 | 0.38 | 0.20 | 0.20 |
| | BS-80-01-09S(3)S | 0.90 | 0.47 | 0.24 | 0.31 |
| Kuang and Wong 2005 | NSD-200 | 2.79 | 0.63 | 0.33 | 0.44 |

| Reference | Unit | $f_{cu}$ (MPa) | $f_y$ (MPa) | $f_{yh}$ (MPa) |
|---|---|---|---|---|
| Walls | | | | |
| Wong 2005 | W1 | 58.8 | 423.0 | 364 |
| | W2 | 50.9 | 431.0 | 423 |
| Kuang and Ho 2007 | UD-1.0 | 38.0 | 520.0 | 520 |
| | UD-1.5 | 43.6 | 520.0 | 520 |
| | CD-1.0 | 39.1 | 520.0 | 520 |
| | CD-1.5 | 42.2 | 520.0 | 520 |
| Columns | | | | |
| Xiong 2001 | X1 | 51.2 | 510 | 410 |
| | X2 | 55.3 | 510 | 410 |
| | X7 | 51.1 | 510 | 410 |
| Huang 2003 | E-0.0 | 43.1 | 513 | 361 |
| | E-0.3 | 46.1 | 558 | 406 |
| Lam et al. 2003 | X-7 | 47 | 433 | 273 |
| | X-9 | 47 | 418 | 273 |
| Li 2003 | E-C80-B80-0 | 88.2 | 557 | 374 |
| | E-C80-B40-0.2 | 87.2 | 557 | 374 |
| Ho 2003 | BS-60-06-61S | 56.5 | 525 | 378 |
| | BS-60-06-61C | 60.4 | 525 | 357 |
| | BS-100-03-24S | 95.1 | 522 | 357 |
| | BS-100-03-24C | 109.5 | 522 | 357 |
| | BS-80-01-09S(1) | 89.6 | 531 | 378 |
| | BS-80-01-09S(2) | 85.4 | 531 | 357 |
| | BS-80-01-09S(3)S | 83.2 | 531 | 367 |
| Kuang and Wong 2005 | NSD-200 | 34.2 | 520 | 365 |

$$\theta_y = \Delta_y / l \tag{9}$$

$$\theta_u = \Delta_u / l \tag{10}$$

where $l$ is the length of shear span of the specimens.

The yield and ultimate drift ratios as obtained from the experimental testings are summarized in Table 4. The following important observations are made: (i) the lateral load resisting elements (comprising both the columns and walls) possesses a minimum drift ratio of 0.39% at yield and 0.88% at ultimate conditions, (ii) the axial load ratio is critical to the ductility of the member, and (iii) the shear span-to-depth ratio ($m$) is apparently also critical to the yield drift ratio $\theta_y$. For example, short columns with very low shear span ($m$ less than 1.5), can have $\theta_y$ reduced to the very low level of ~0.4%, regardless of the axial load ratio. When the axial load ratio ($n$) exceeds 0.4, the drift ductility factor can be as low as 2.1 (due possibly to the relative low transverse steel ratios of $\rho_{sh}$<0.53 in the columns and $\rho_{sh}$<0.92 in the wall panels). For columns with $m$ greater than 1.5 (which represent the great majority of cases) the yield drift ratio $\theta_y$ is at least 0.78 % and the ultimate drift ratio $\theta_u$ is at least 1.5 % irrespective of the axial load ratio. The presence of transverse reinforcement does not seem to have any significant influences on the yield drift ratios nor the ultimate drift ratios.

The limit of both the yield and ultimate drift angles for walls is generally lower than columns, but this does not mean that walls are more critical since the geometrical stability of walls in the in-plane direction is a significant reserve which is not represented by the face value of $\theta_u$. Furthermore, the lateral stiffness of shear walls with small shear span-to-depth ratio ($m$<1.5) is relatively high and the natural period of the building composed of those walls as the main lateral supports is usually short. This type of buildings is likely to be strength controlled rather than displacement or drift controlled under a seismic attack. Thus, columns are considered to be more critical than walls in spite of the results shown in Table 4.

It is noted that the predicted ultimate drift ratio is based on a 20% degradation in strength which has been used as the criterion to define the condition of ultimate behaviour (refer Figure 3). It is noted that in conditions of moderate ground shaking generated by small-medium magnitude earthquakes (M<7), the horizontal strength demand of the earthquake on a lateral load resisting element is not sustained when the element is subject to large displacement causing a degradation in strength and/or stiffnesses of the column. In such conditions, a column can be well within the condition of ultimate stability in an earthquake and hence is able to continue carrying the de-

signed gravity loading even though its lateral strength has degraded by more than 20%. The ability of a wall or column to continue carrying the full gravity loading at large displacement (as opposed to a 20% degradation in strength) can be used as the alternative criterion for defining the ultimate angle of drift in the context of seismic performance evaluation of structures in regions of low-to-moderate seismicity like Hong Kong.

A collapse model for RC columns and walls based on stability at large displacement is still under development by the authors. It has been shown in the pilot research undertaken at the University of Melbourne on RC columns (with widely spaced stirrups) that column specimens were capable of sustaining the full designed gravity loading when the drift ratio has exceeded 2% (Rodsin *et al*, 2006). In spite of this, seismic performance evaluation as presented in the rest of this paper will still be based on the conventional (and the much more conservative) criteria of ultimate failure. For example, the minimum ultimate angle of drift will still be taken as 1.5% according to Table 4. The conservatism of such estimates should be noted.

An attempt has been made to correlate test data for different structural members, namely, wall panels and columns, by a single mathematical expression. After examining several mathematical formulations, non-dimensional parameter $\gamma$ were introduced to include the influences due to the variations in the geometric and material properties.

$$\gamma = (1+m)^{0.27}(b/d)^{0.02} \cdot 0.55^{n} \cdot 1.5^{\rho_s f_y / f_{cu}} \qquad (11)$$

Empirical equation (12) was developed by regression analysis for the estimation of the yield drift ratio for both the columns and walls.

$$\theta_y = 2.02\gamma - 1.88 \ [\%]; \qquad R^2=0.86 \qquad (12)$$

The $R^2$ value is higher than 0.8 indicating very good correlations between the predicted and measured values. The above empirical equation would not be applicable to conditions where the axial load ratio $n \geq 0.35$ or the shear span-to-depth ratio $m \leq 1.5$ due to the lack of test data.

The model of Panagiotakos and Fardis (2001) which was based on 633 cyclic tests data of columns and walls is defined by equation (13) for estimation of the ultimate drift ratio.

$$\theta_u = \alpha_{st,cyc}\left(1+\frac{a_{st}}{2}\right)(1-0.4\alpha_{wall})(0.2^{n}) \left(f_c'\right)^{0.175} m^{0.4} 1.1^{\left(\alpha\rho_{sh}\frac{f_{yh}}{f_c'}\right)} \qquad (13)$$

where $\alpha_{st,cyc}$ is the coefficient for the type of steel and equal to 1.125 for hot-rolled ductile steel, $\alpha_{st}$ is the coefficient of slip and equal to 1 if there is slippage of the longitudinal bars from their anchorage beyond the section of maximum moment, or 0 if there is not, and $\alpha_{wall}$ is the coefficient equal to 1 for shear walls and 0 for columns. The concrete cylinder strength $f_c'$ may be taken as $0.8f_{cu}$. Figure 4 shows a comparison between the predicted ultimate drift ratios by equation (13) and the measured ultimate drift ratios from Table 4 and reasonably good agreements of both results are observed.

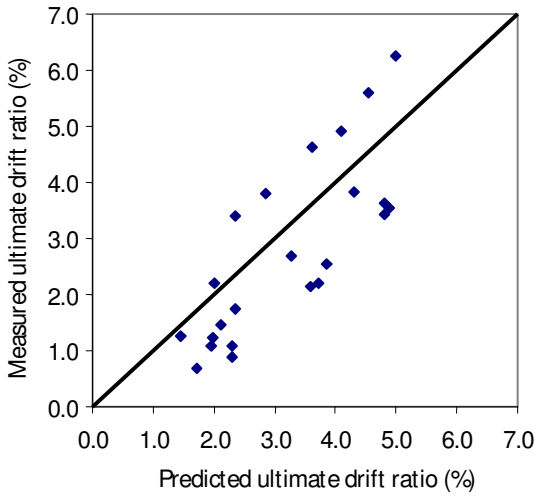


Figure 4. Comparison between the predicted and measured ultimate drift ratios.

Table 4. Summary of yield and ultimate drift ratios of the specimens.

| Unit | Yield drift ratio (%) | Ultimate drift ratio (%) |
|---|---|---|
| Wall | | |
| W1 | 0.72 | 2.21 |
| W2 | 0.61 | 1.25 |
| UD-1.0 | 0.39 | 1.23 |
| UD-1.5 | 0.42 | 1.10 |
| CD-1.0 | 0.46 | 1.10 |
| CD-1.5 | 0.41 | 0.88 |
| Column | | |
| X1 | 0.78 | 2.68 |
| X2 | 0.88 | 4.92 |
| X7 | 1.20 | 3.82 |
| E-0.0 | 1.81 | 5.60 |
| E-0.3 | 1.24 | 3.79 |
| X-7 | 0.74 | 1.46 |
| X-9 | 0.35 | 0.69 |
| E-C80-B80-0 | 1.72 | 6.27 |
| E-C80-B40-0.2 | 1.12 | 4.62 |
| BS-60-06-61S | 1.10 | 1.75 |
| BS-60-06-61C | 1.15 | 3.40 |
| BS-100-03-24S | 1.15 | 2.54 |
| BS-100-03-24C | 1.15 | 2.20 |
| BS-80-01-09S(1) | 1.20 | 3.53 |
| BS-80-01-09S(2) | 1.30 | 3.63 |
| BS-80-01-09S(3)S | 1.25 | 3.44 |
| NSD-200 | 1.12 | 2.15 |

### 2.5 *Stiffness degradation and damping ratio*

Mass, stiffness and damping ratios are the three fundamental parameters controlling the dynamic response behaviour of the structure. When subject to earthquake ground shaking, the mass of a building may be treated as constant with respect to time, or ductility. However, the stiffness and damping ratio would normally vary with the drift demand (or ductility demand). The initial lateral stiffness $K_o$ of the member is defined as the secant stiffness based on the condition at one-third of the ultimate drift capacity. Recent investigation by the authors based on observations of cyclic load testing of RC columns revealed that the secant lateral stiffness $K_i$ of the column is reduced by some 40-60% from the initial lateral stiffness $K_o$ when the condition of notional yield is reached (i.e. $\theta_i = \theta_y$, $\mu = 1$). Meanwhile, the equivalent viscous damping is estimated at around 5-13% (averaged at 8-9%). As the drift demand is increased beyond yield, the value of $K_i$ will continue to reduce to a very low level whilst the averaged value of damping will increase to about 10-13% as the drift demand is double, and triple, of that at yield. These recent findings from the parametric studies of RC columns undertaken by the authors are summarised in Table 5.

Table 5. Averaged secant stiffness and equivalent viscous damping.

| $\mu$ | 0 | 1 | 1.5 | 2 | 2.5 | 3 |
|---|---|---|---|---|---|---|
| $K_i$ (% of $K_o$) | 100% | 48% | 33% | 22% | 16% | 11% |
| $\zeta_e$ (% of critical) | 0 | 8-9% | 10% | 11% | 12% | 13% |

In a building frame where inelastic behaviour is experienced locally by some of the columns, the overall degradation in stiffness and equivalent viscous damping of the frame as a whole can be much less than that shown in Table 5. This is because the tabulated figures for stiffness degradation and damping were based on the behaviour of the column in isolation. Thus, the presented estimates must be properly adjusted before they can be used as the global stiffness degradation and global damping of a building.

## 3 INTER-STOREY DRIFT DEMAND OF BUILDINGS IN HONG KONG

Seismic assessment of the existing building stock in low-to-moderate seismic regions presents a unique challenge. It is because the codified empirical factors such as the structural response modification factors cannot be assumed to be applicable to existing buildings which have not been designed and detailed in accordance with the seismic code. Furthermore, design procedures established in high seismic regions are not necessarily effective assessment tools for low-to-moderate seismic regions. Extensive researches have been conducted in Hong Kong and Australia to develop an expeditious yet accurate method to assess the potential seismic drift demands of existing buildings (which are without seismic design considerations). This method can also be extended to the assessment of seismically designed buildings provided that the dynamic drift factors (described in Section 3.4) have been properly calibrated.

### 3.1 *Design response spectra of Hong Kong*

To correctly estimate the seismic drift demands of existing buildings, accurate response spectra and precise natural period prediction formula should be used. Design response spectra based on Chinese Code GB50011-2001 (2001) and the uniform hazard response spectrum developed at the University of Hong Kong (HKU) for rock sites (Tsang 2006) are shown in Figure 5. Earthquake scenarios with a 2% probability of exceedance in 50 years have been considered. Detailed geological information of the site has been presented in Tsang (2006). The acceleration response spectra of Figure 5 and the displacement response spectra of Figure 6 include predictions for rock sites and the more onerous soil sites (Tsang *et al*. 2006). The spectral displacement demand stipulated by the Chinese Code GB50011-2001 (2001) features indefinite increasing in values with increasing natural period ($T$) when $T > 2$ sec, which does not take into account the maximum magnitude limit of the projected earthquake scenarios. The more realistic displacement-based response spectra developed by HKU (which features an upper bound displacement demand) have been used in this study for the prediction of the seismic drift demand.

It is further noted that the site-specific displacement response spectra shown on Figure 6 (based on deterministic analyses) can be much more conservative than that shown by the *Uniform Hazard Response Spectra* (UHRS) for the same probability of exceedance. In the construction of UHRS of a site class, response spectra analysed for a multitude of earthquake scenarios and for sites possessing different site natural period (where high amplification is typically featured) are averaged. This averaging can result in understating the peak displacement demand on an onerous site when subject to an onerous earthquake scenario. In view of this, the more conservative response spectrum obtained from a site/scenario-specific analysis at *Tseung Kwan O* was taken to benchmark the seismic demand on Hong Kong soil sites. This response spectrum features a maximum displacement demand of about 120 mm for natural period exceeding 1.6 – 1.7 sec. Lin-

ear interpolation can be used to estimate the spectral displacement demand (*RSD*) for lower natural periods. For example, a *RSD* value of 60 mm is predicted for a natural period of 0.8 sec.

### 3.2 *Effective natural period of existing RC buildings in Hong Kong*

Su *et al*. (2005) conducted a comprehensive investigation of the natural vibration period of existing RC buildings in Hong Kong. Ambient vibration test were carried out to measure the natural periods of existing buildings with height ranging from 50m to around 400m. The measured natural periods are summarized in Figure 7.

It was found that the natural periods of the buildings in Hong Kong can be conveniently quantified by the following simple expressions:

Upper bound: $T_1 = 0.020H_b$ (14a)

Average: $T_1 = 0.015H_b$ (14b)

Lower bound: $T_1 = 0.010H_b$ (14c)

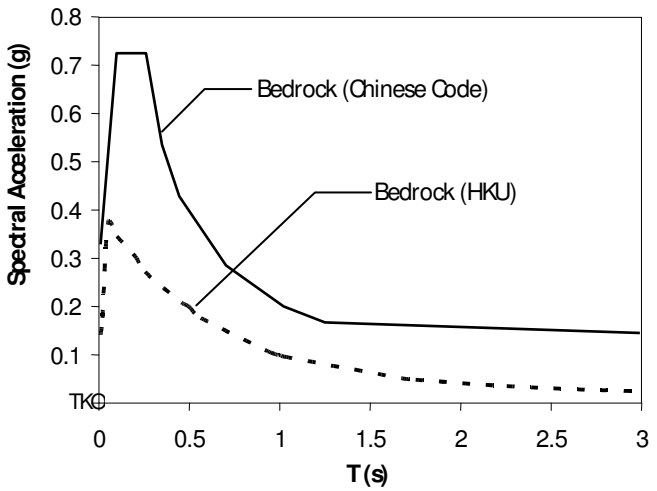


Figure 5. Design acceleration response spectra (2% probability of exceedance in 50 years and damping ratio =5%).

It is noted that the fundamental period ($T_1$) of the buildings are considerably smaller than estimates obtained from the empirical model of IBC-2006 (ICC 2006) and AS/NZS 1170.4 (2007). This can be explained by the fact that buildings in Hong Kong are designed with much higher lateral loads compared to that for similar structures designed in the United States, Australia or Europe. Consequently, tall buildings in Hong Kong are normally constructed of stiffer structural forms, such as shear walls or core walls arrangement, as opposed to flexible moment resisting frames.

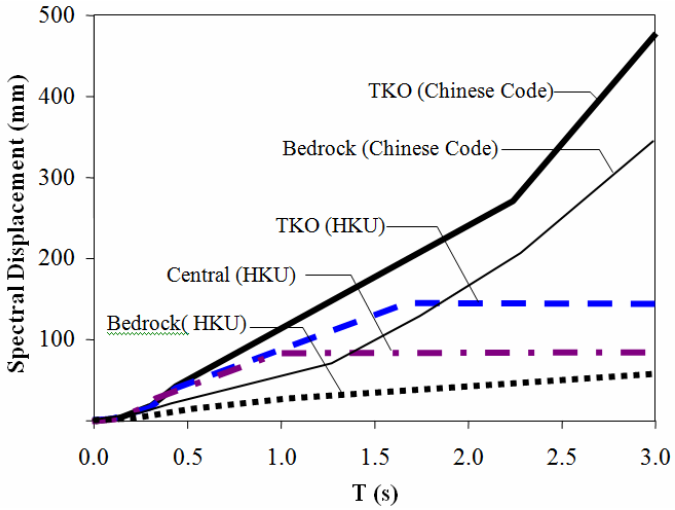


Figure 6. Design displacement response spectra (2% probability of exceedance in 50 years and damping ratio = 5%).

Thus, the fundamental period is generally lower for Hong Kong buildings even though the walls are more massive (Su *et al*. 2003). Sheikh (2005) used a commercial structural program to estimate the natural periods for the second and third modes of vibration ($T_2$ and $T_3$ respectively) and proposed the following relationships:

$$T_2 = 0.25T_1 \quad \text{and} \quad T_3 = 0.125T_1 \tag{15}$$

The relationships of equation (15) are comparable with that proposed by Lagomarsino (1993) which was based on measurements from 52 RC buildings measured in Italy.

Equations (14)–(15) enable the initial lateral stiffness of real buildings to be estimated by back calculations. By combining this with the stiffness and damping models introduced in Section 2.5 (and summarised in Table 5), the drift dependent stiffness and damping properties of the building can be estimated. Under seismic actions, buildings would undergo inelastic deformation due to, for instance, flexural cracking of concrete and yielding of reinforcement. As illustrated in Section 2, the secant lateral stiffness decreases with increase in ductility.

It is noted that the realistic modelling of the as-constructed building is never complete without taking into account influences by the non-structural components which include facades and partitions (particularly those extending the full height of the floor and connected to the ceiling). Unfortunately, only a few studies have been devoted to the investigation of the degradation in the lateral stiffness of non-structural components in buildings. Whilst there is on-going investigation into the stiffness behaviour of non-structural components, a parabolic relationship as defined by equation (16) has been adopted for modelling in this study.

$$\frac{K_{ni}(\mu)}{K_{no}} = g(\mu) = \begin{cases} 1-\mu^2/4 & \mu \le 2 \\ 0 & \mu > 2 \end{cases} \quad (16)$$

where $K_{no}$ and $K_{ni}$ are the lateral stiffnesses of non-structural components at $\mu$ equal to zero and $\mu$ greater than zero respectively.

The stiffness degradation model of equation (16) is expected to result in a conservative estimate of the degradation in stiffness of the building and consequently a conservative estimate of the drift demand on the building as a whole.

Equation (16) features maximum tangential stiffness at $\mu$=0 and zero tangential stiffness at $\mu$=2. Su *et al.* (2005) employed ambient vibration tests to measure three frame-and-wall buildings in Hong Kong. From numerical calibrations, it was revealed that the non-structural components such as partitions, in-filled walls, parapet beams, finishes, etc. could constitute a very high proportion of lateral stiffness. The ratio ($\beta$) of initial lateral stiffness of non-structural and structural components ranges from 4.5 (for frame structures) to 0.28 (for wall structures).

As distortional deformations (lateral shear deformation for frame structures and curvature deformation for wall structures) are not uniformly distributed along the height of building and higher distortional deformations would concentrate at the lower stories, a factor, $\eta_1$ = 0.8, has been introduced to convert the maximum local lateral stiffness degradation at the base level of the building to the global lateral stiffness degradation. The effective natural period of the building may therefore be approximated by

$$T_{eff} = T_1 \sqrt{\frac{\eta_1(1+\beta)}{f(\mu_{\max}) + \beta g(\mu_{\max})}} \quad (17)$$

where μmax is the maximum displacement/drift ductility factor of the structural component in the building. It is noted that buildings in Hong Kong are usually found on stiff pile foundations. Hence, the rotational effect at foundations is usually small and is neglected in subsequent analyses. According to equation (17), when β = 1, η1 = 0.8, the ductility factor μ = 1 (or 3), the ratio (Teff / T1) would be equal to 1.88 (or 3.36). Clearly such a high period lengthening effect cannot be ignored in non-linear seismic analysis of buildings.

### 3.3 *Methodology for prediction of the inter-storey drift demand*

An expeditious step-by-step procedure for modelling the maximum inter-storey drift demand of existing buildings has been developed in Chandler *et al.* (2002a) and the contributions from higher modes have been considered. With consideration of the period lengthening effects, the method was further applied and presented in Gad *et al.* (2002) and in Chandler *et al.* (2002b). Li (2004) incorporated the effect of variation of damping ratio into the methodology. Sheikh (2005) has further divided the total inter-storey drift ratio into shear drift ratio and flexural drift ratio. Recently, Zhu *et al.* (2007) extended this method to calculate the maximum chord rotation of coupling beams.

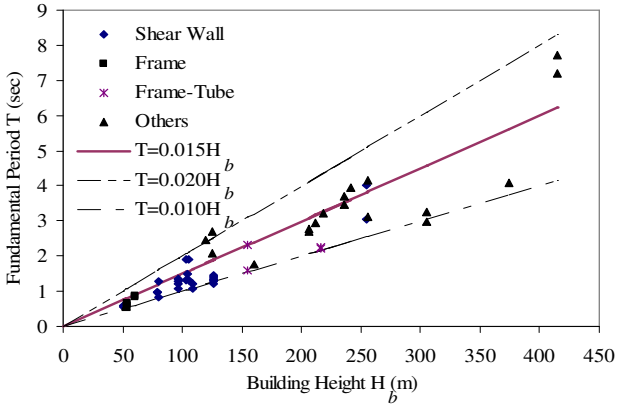


Figure 7. Natural periods of buildings in Hong Kong.

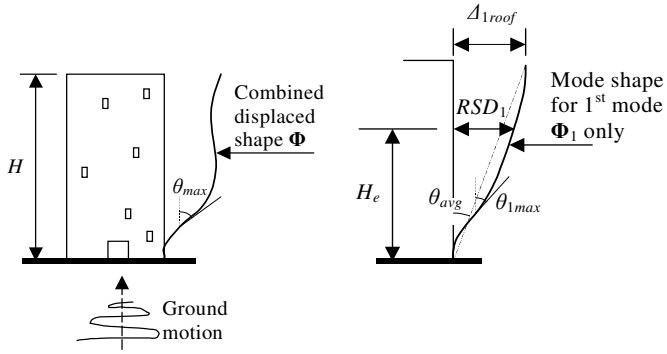


Figure 8. Illustration of drift angles $\theta_{max}$, $\theta_{1max}$, $\theta_{avg}$ .

The methodology developed for expressing building drift demand has been illustrated in Figure 8. The maximum seismic drift angle $\theta_{\max}$ due to the combined vibration modes can be related to the seismic response spectral displacement at the fundamental mode period *RSD*, using equation (18).

$$\theta_{\max} = \lambda_1 \lambda_2 \lambda_3 \frac{RSD(T_{eff})}{H_b} \quad (18)$$

where $H_b$ is the building height and $\lambda_i$ ($i$=1-3) are the dynamic drift coefficients. More specifically, the maximum inter-storey drift angle $\theta_{\max}$ of the building can be related to that of the fundamental lateral vibration mode by the higher mode dynamic coefficient which is defined by equation (19).

$$\lambda_2 = \frac{\theta_{\max}}{\theta_{1\max}} \tag{19}$$

in which the subscript '1' denote the fundamental vibration mode. The maximum inter-storey drift angle of the fundamental mode $\theta_{1\max}$ may be related to the average drift angle $\theta_{1avg}$ ($=\Delta_{1roof}/H_b$) by the drift coefficient $\lambda_1$ which is defined by equation (20).

$$\lambda_1 = \frac{\theta_{1\max}}{\theta_{1avg}} \tag{20}$$

Furthermore, the lateral displacement at roof level $\Delta_{1roof}$ can be obtained from $RSD(T_{eff})$ by equation (21).

$$\lambda_3 = \frac{\Delta_{1roof}}{RSD(T_{eff})} \tag{21}$$

By substituting equations (19) - (21) into equation (18) and denoting the combined dynamic drift coefficient as $\lambda_{\max} = \lambda_1\lambda_2\lambda_3$, equation (18) may be re-written as equation (22)

$$\theta_{\max} = \lambda_{\max}\frac{RSD(T_{eff})}{H_b} \tag{22}$$

The combined dynamic drift coefficient can be considered to be composed of the higher mode effects ($\lambda_2$) and the fundamental mode effects ($\lambda_1$ and $\lambda_3$). All the drift coefficients have been calibrated by Li (2004), Sheikh (2005) and Zhu (2006) using response spectrum analysis of typical buildings with a wide range of heights and types. The drift factors are found to be $\lambda_1 \approx 1.5$, $\lambda_2 = 1.0$ and $\lambda_3 \approx 1.5$ based on the uniform hazard response spectrum.

Depending on the magnitude of the maximum drift demand, modification for potential inelastic effects has been implemented. The effective (or equivalent) damping ratio of the entire building may be estimated using Table 5 and the corresponding ductility factor can be obtained using equation (23).

$$\mu = \frac{\theta_{\max}}{\theta_y} \tag{23}$$

Note that the response spectra in Figures 5 and 6 are based on the 5% level of damping. The demand response spectrum should then be modified, for the effective damping ratio, using the damping modification factor (*DMF*) as defined by equation (24) according to Eurocode 8 (2005):

$$DMF = \sqrt{\frac{10}{5+\eta_2\varsigma_e}} \tag{24}$$

To take into account the non-uniform distribution of damping along the height of the building, a factor, $\eta_2 = 0.8$, is introduced to convert the maximum damping ratio of structural components (at the base level of the building) to the ratio for global structural damping. As parameters estimated from equations (23) and (24) and Table 5 depend on the predetermined value for $\theta_{\max}$ [equation (22)], iteration is required. It has been found that three such iterations are sufficient for the result to converge.

### 3.4 *Prediction of the inter-storey drift demand*

As mentioned in Section 2, yield drift ratio is dependent on various materials used in the structure, their loading and geometric properties. The parameter values listed in Table 6 have been assumed for the determination of the average and minimum yield drift ratios for the wall and column members in a typical Hong Kong building. It can be seen from Table 4 that the yield drift ratio ranges from 0.35 to 1.81. For columns with shear span-to-depth ratios greater than 3, the yield drift ratio is constrained to the much narrower range of 0.8 – 1.2 (with a few exceptions, see Tables 4 and 6). This latter range of $\theta_y$ has been adopted for predicting the inter-storey drift demand of existing buildings in Hong Kong. It is found that the drift demands demonstrate very limited variation with different $\theta_y$, hence only one set of results (based on a conservative estimate of $\theta_y$ = 0.75) is presented in Figure 9.

Table 6. Parameters used for determination of yield and ultimate drift ratios.

| Unit | Geometric and Loading Properties | | | | |
|---|---|---|---|---|---|
| | *M* | *b/d* | *n* | $\rho_s$(%) | $\rho_{sh}$(%) |
| Column | | | | | |
| Average | 5.0 | 1 | 0.3 | 3.0 | 0.3 |
| Minimum | 3.0 | 1 | 0.5 | 3.0 | 0.3 |
| Wall | | | | | |
| Average | 4.0 | 0.02 | 0.30 | 1.5 | 0.6 |
| Minimum | 2.0 | 0.02 | 0.30 | 3.0 | 0.6 |

| Unit | Material Properties | | | $\theta_y$ (%) | $\theta_u$ (%) |
|---|---|---|---|---|---|
| | $f_{cu}$ (MPa) | $f_y$ (MPa) | $f_{yh}$ (MPa) | | |
| Column | | | | | |
| Average | 35 | 460 | 460 | 1.33 | 4.49 |
| Minimum | 35 | 460 | 460 | 0.68 | 3.18 |
| Wall | | | | | |
| Average | 35 | 460 | 460 | 0.73 | 2.06 |
| Minimum | 35 | 460 | 460 | 0.58 | 1.56 |

* $\alpha$ assumed to be 0.2 for walls and 0.3 for columns, and $\alpha_{st}$ are 0.5 and 0.0 for columns and walls respectively.

The effective natural period of structures is obtained using the predictive relationships of Table 5 and equation (17) together with equations (14b) and (16). The non-linear damping effects were also modelled using Table 5 and equations (23) and (24). The

calculated maximum inter-storey drift demands on buildings are shown in Figure 9 for a 2% probability of exceedance in 50 years (return period of approximately 2500 years). It is shown that inter-storey drift demands on soil sites are much higher than that on rock sites. The maximum drift demands associated with the rare earthquake scenarios on deep soil sites were predicted to be around 0.3%. Low to medium-rise buildings with height less than 120m would experience higher seismic demand.

When compares the estimated maximum inter-storey drift demands of 0.3% with the minimum drift capacity (~1.5%) of vertical supporting elements, the drift capacity is in general higher than the demand by a factor of 5. Hence, existing buildings in Hong Kong (located on both rock and deep soil sites) are unlikely to be subject to significant drift-induced damage in rare earthquake scenarios consistent with a 2% probability of exceedance in 50 years (or return period of approximately 2500 years). In fact, the maximum inter-storey drift demand (0.3%) is less than any of the yield drift ratios of lateral resisting elements listed in Table 4. Hence, elastic analyses, e.g. response spectrum analysis based on the notional 5% damping would be sufficiently accurate for routine seismic design and assessment of typical RC buildings in Hong Kong. The accuracies of the presented degradation and damping models are therefore not critical to the results of the assessment.

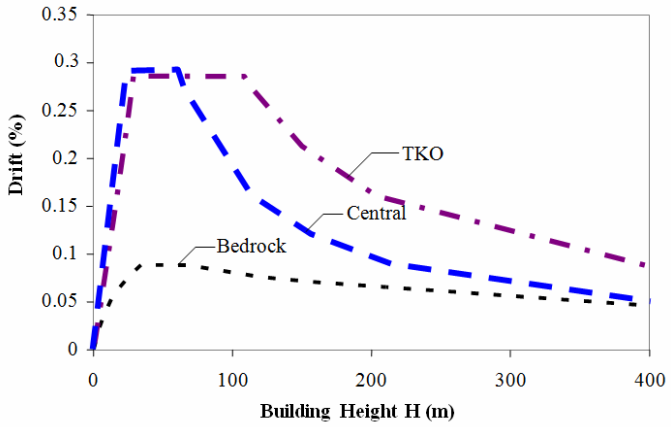


Figure 9. Maximum inter-storey drift demand of buildings in Hong Kong (2% probability of exceedance in 50 years).

It is, however, noted that the evaluation presented so far has not considered buildings with a soft-storey, and torsional irregularity which warrants special attention in view of their seismic vulnerability. It is possible that in a soft-storey building the response spectral displacement demand (as shown in Figure 6) may be localised to just one single-storey. Considering cases where the height of the soft-storey is 4 m whilst noting that the ultimate drift capacity of RC columns supporting the soft-storey is 1.5% (refer Section 2.4), the limiting value of *RSD* is accordingly equal to 60 mm. From the displacement spectrum diagram presented in Figure 6 for the onerous soil site of *Tseung Kwan O*, this value of *RSD* is reached when the natural period of the building exceeds 0.6 – 0.7 sec. This natural period limit is translated to a building height of about 45 m (based on equation 14b or Figure 7). Thus, seismically induced collapse of the soft-storey is unlikely if the height of the building is within 45 m (which corresponds to 14-16 storeys). In other words, buildings in Hong Kong are expected to be structurally safe provided that buildings exceeding 14-16 storeys found on a flexible soil site do not have a soft-storey (i.e. floors are all braced adequately by core walls or shear walls).

## 4 CONCLUSIONS

A comprehensive study of the seismic inter-storey drift demand and capacity of building structures in Hong Kong has been presented. The research findings are summarized as follows:

(1) According to the site-specific response spectra developed at HKU, the maximum inter-storey drift demand at deep soil sites in Hong Kong in conditions of rare earthquake events with 2% probability of exceedance in a 50 year design life (return period of approximately 2500 years) is around 0.3% for regular buildings without soft-storey and torsional irregularity.

(2) The limit of yield drift of columns is normally higher than 0.8% and limit of ultimate drift is normally higher than 1.5% except for columns with low shear span-to-depth ratios ($m \leq 3$). Walls are considered to be less critical in spite of the lower limits reported.

(3) Collapse of beam-column frame structures or wall structures under earthquake-induced load is therefore unlikely except for buildings exceeding 45 m in height (14-16 storeys), have a soft-storey feature and located in a deep soft soil site. The condition of yield is unlikely to be reached in buildings without a soft-storey.

(4) RC structures, particular for those with high axial load ratio (> 0.4) and located at soil sites could be slightly damaged under a rare earthquake event.

(5) Excessive inter-storey drift may result in moderate damage of brittle non-structural components. (e.g. glass or stone cladding)

(6) Elastic analyses e.g. response spectrum analysis should be sufficiently accurate for routine seismic design and assessment of typical RC buildings in Hong Kong.

## 5 ACKNOWLEDGEMENTS

The research described here has been supported by the Research Grants Council of Hong Kong SAR (Project Nos. HKU7129/03E and HKU7168/06E).

## REFERENCES

AS/NZS 1170.4 (2007). Australian / New Zealand Standard for Structural Design Actions, Part 4: Earthquake Actions in Australia. Standards Australia and Standards New Zealand.

BD (2004). Code of Practice for Structural Use of Concrete 2004, Hong Kong, Buildings Department, The Government of the Hong Kong Special Administrative Region.

BSI (1985). BS8110 The Structural Use of Concrete: Part I, Code of Practice for Design and Construction. London, British Standards Institution.

BSI (1972). CP110, Code of Practice for the Structural Use of Concrete. London, British Standards Institution.

BSI (1969). CP114, Code of Practice for the Structural Use of Reinforced Concrete in Buildings. London, British Standards Institution.

Chandler, A.M., Su, R.K.L. and Lee, P.K.K. (2002a). Seismic Drift Assessment for Hong Kong Buildings. Recent Developments in Earthquake Engineering, Annual Seminar 2001/02, The Hong Kong Institution of Engineers Structural Division and The Institution of Structural Engineers (HK Division), 17 May, 1-15.

Chandler, A.M., Su, R.K.L. and Sheikh, M.N. (2002b). Drift-Based Seismic Assessment of Buildings in Hong Kong, Proceedings of International Conference on Advances and New Challenges in Earthquake Engineering Research (ICANCEER 2002), 15-20 August, Harbin and Hong Kong, CHINA, 3, 257-265.

Eurocode 8 (EC8) (2005). BS EN 1998-1:2005. Design of Structures for Earthquake Resistance. General Rules, Seismic Actions and Rules for Buildings.

Gad, E.F., Lam, N.T.K., Duffield, C.F., Hira, A. and Chandler, A.M. (2002). Seismic Behaviour of Non-Structural Components in High-Rise Buildings. Proceedings of the 12th European Conference on Earthquake Engineering, September 9-13, Barbican Centre, London, UK.

GB50011-2001 (2001). Code for Seismic Design of Buildings, PRC, Building Industry Press.

Ho, J.C.M. (2003). Inelastic Design of Reinforced Concrete Beams and Limited Ductile High-Strength Concrete Columns, PhD Thesis, The University of Hong Kong.

Kuang, J.S. and Ho, Y.B. (2007). Inherent Ductility of Non-seismically Designed and Detailed Reinforced Concrete Shear Walls, Transactions of The Hong Kong Institution of Engineers, 14(1), 7-12.

Huang, K. (2003). Design and Detailing of Diagonally Reinforced Interior Beam-Column Joints for Moderate Seismicity, PhD Thesis, The University of Hong Kong.

International Code Council (ICC). (2006). International Building Code IBC-2006, ICC, USA.

Kuang, J.S. and Wong, H.F. (2005), Improving Ductility of Non-Seismically Designed RC Columns, Proceedings of the Institution of Civil Engineers Structures and Building. 158 (4), 13-20.

Lagomarsino S (1993) Forecast Models for Damping and Vibration Periods of Buildings, Journal of Wind Engineering and Industrial Aerodynamics, 48(2-3), 221-239.

Lam, S.S.E., Wu, B., Wong, Y.L., Wang, Z.Y., Liu, Z.Q. and Li, C.S. (2003). Drift Capacity of Rectangular Reinforced Concrete Columns with Low Lateral Confinement and High-Axial Load, Journal of Structural Engineering. ASCE 129(6), 733-741.

Li, J. (2003). Effects of Diagonal Steel Bars on Performance of Interior Beam-Column Joints Constructed with High-Strength Concrete, PhD Thesis, The University of Hong Kong.

Li, J.H. (2004). Seismic Drift Assessment of Buildings in Hong Kong with Particular Application to Transfer Structures, PhD Thesis, The University of Hong Kong

Panagiotakos, T.B. and Fardis, M.N. (2001). Deformations of Reinforced Concrete Members at Yielding and Ultimate, ACI Structural Journal, 98(2), 135-148.

Paulay, T. and Priestley, M.J.N. (1992). Seismic Design of Reinforced Concrete Masonry Buildings, New York, John Wiley & Sons.

Priestley, M.J.N (2000), Performance Based Seismic Design, Bulletin of the New Zealand National Society of Earthquake Engineering, 33(3), 325-346.

Rodsin, K, Lam, N.T.K., Wilson, J.L. and Goldsworthy, H. (2006). The collapse behaviour of columns with a low aspect ratio, Proceedings of the 19th Australasian Conference of Mechanics of Solids and Materials, University of Canterbury, Christchurch, New Zealand. Paper no. 181.

Sheikh, M.N. (2005), Seismic Assessment of Buildings in Hong Kong with Special Emphasis on Displacement-Based Approaches, PhD Thesis, The University of Hong Kong.

Sheikh, S.A. and Uzumeri, S.M. (1982) Analytical model for concrete confinement in tied columns, Journal of the Structural Division, ASCE, 108, ST12, 2703-2722.

Su, R.K.L., Chandler, A.M. and Wong, P.C.W. (2001). Construction of Seismic Reinforced Concrete Details in Hong Kong, Proceedings of International Conference on Construction, Vol. 2, Hong Kong, 19-21 June 2001, 196-205.

Su, R.K.L., Chandler, A.M., Lee, P.K.K., To, A.P. and Li, J.H. (2003). Dynamic Testing and Modelling of Existing Buildings in Hong Kong, Transactions of Hong Kong Institution of Engineers, 10(2), 17-25.

Su, R.K.L., Chandler, A.M., Sheikh, M.N. and Lam, N.T.K. (2005). Influence of Non-Structural Components on Lateral Stiffness of Tall Buildings, Structural Design of Tall and Special Buildings, 14(2), 143-164.

Su, R.K.L. and Wong, S.M. (2007). A Survey on Axial Load Ratios of Structural Walls in Medium-rise Residential Buildings in Hong Kong, Transactions of The Hong Kong Institution of Engineers 14 (3), 40-46.

Tsang, H.H. (2006). Probability Seismic Hazard Assessment: Direct Amplitude-Based Approach, PhD Thesis, The University of Hong Kong.

Tsang HH, Chandler A.M, Lam NTK. (2006). Estimating nonlinear site response by single period approximation. Earthquake Engineering and Structural Dynamics. Volume 35, No 9, pp.1053-1076.

Wong, S.M. (2005). Seismic Performance of Reinforced Concrete Wall Structures under High Axial Load with Particular Application to Low-to-Moderate Seismic Regions, MPhil Thesis, The University of Hong Kong.

Xiong, Z.H. (2001). Reinforced Concrete Column Behaviour Under Cyclic Loading. PhD Thesis, The University of Hong Kong.

Zhu, Y. (2006). Retrofitting Reinforced Concrete Coupling Beams by Bolted Side Plates for Strength and Deformability, PhD Thesis, The University of Hong Kong.

Zhu, Y., Su. R.K.L. and Zhou, F.L. (2007). Cursory Seismic Drift Assessment for Buildings in Moderate Seismicity Regions. Earthquake Engineering and Engineering Vibration. 6(1), 85-97.